

1 **Evolutionary parallelisms of pectoral and pelvic network-anatomy from fins to limbs**

2
3 Borja Esteve-Altava^{1*}, Stephanie E. Pierce², Julia L. Molnar³, Peter Johnston⁴, Rui Diogo⁵, John R.
4 Hutchinson¹
5

6 **Affiliations**

7 1. Structure & Motion Lab, Department of Comparative Biomedical Sciences, Royal Veterinary
8 College, London, UK.

9 2. Museum of Comparative Zoology and Department of Organismic and Evolutionary Biology,
10 Harvard University, Cambridge, MA, USA.

11 3. Department of Anatomy, New York Institute of Technology, New York, NY, USA.

12 4. Department of Anatomy and Medical Imaging, University of Auckland, New Zealand.

13 5. Department of Anatomy, College of Medicine, Howard University, Washington, DC, USA.

14 * Corresponding author: Borja Esteve-Altava, Structure & Motion Lab, Comparative Biomedical
15 Sciences, Royal Veterinary College, Hatfield, AL9 7TA, UK. email: boresal@gmail.com

16
17 **ABSTRACT**—Pectoral and pelvic lobe-fins transformed into fore- and hindlimbs during the
18 Devonian period, enabling the water-to-land transition in tetrapods. In the timespan of ~60 million
19 years, transitional forms evolved, spanning a wide range of morphologies. Here we traced the
20 evolution of well-articulated appendicular skeletons across the fins-to-limbs transition, using a
21 network-based approach and phylogenetic tools to quantify and compare topological features of
22 skeletal anatomy of fins and limbs. We show that the topological arrangement of bones in the
23 pectoral and pelvic appendages evolved in parallel during the fins-to-limbs transition, occupying
24 overlapping regions of the morphospace, following a directional mode of evolution, and decreasing
25 their disparity over time. We identify the presence of digits as the morphological novelty triggering
26 significant topological changes that clearly discriminated limbs from fins. The origin of digits
27 caused an evolutionary shift towards appendages that were less densely and heterogeneously
28 connected, but more assortative and modular. Topological disparity likewise decreased for both
29 appendages: for the pectoral appendage, until the origin of amniotes; for the pelvic appendage, until
30 a time concomitant with the earliest-known tetrapod tracks. Finally, we tested and rejected the
31 presence of a pectoral-pelvic similarity bottleneck for the network-anatomy of appendages at the
32 origin of tetrapods. We interpret our findings in the context of a dynamic compromise between
33 possibly different functional demands in pectoral and pelvic appendages during the water-to-land
34 transition and a shared developmental program constraining the evolvability of limbs.

35

36

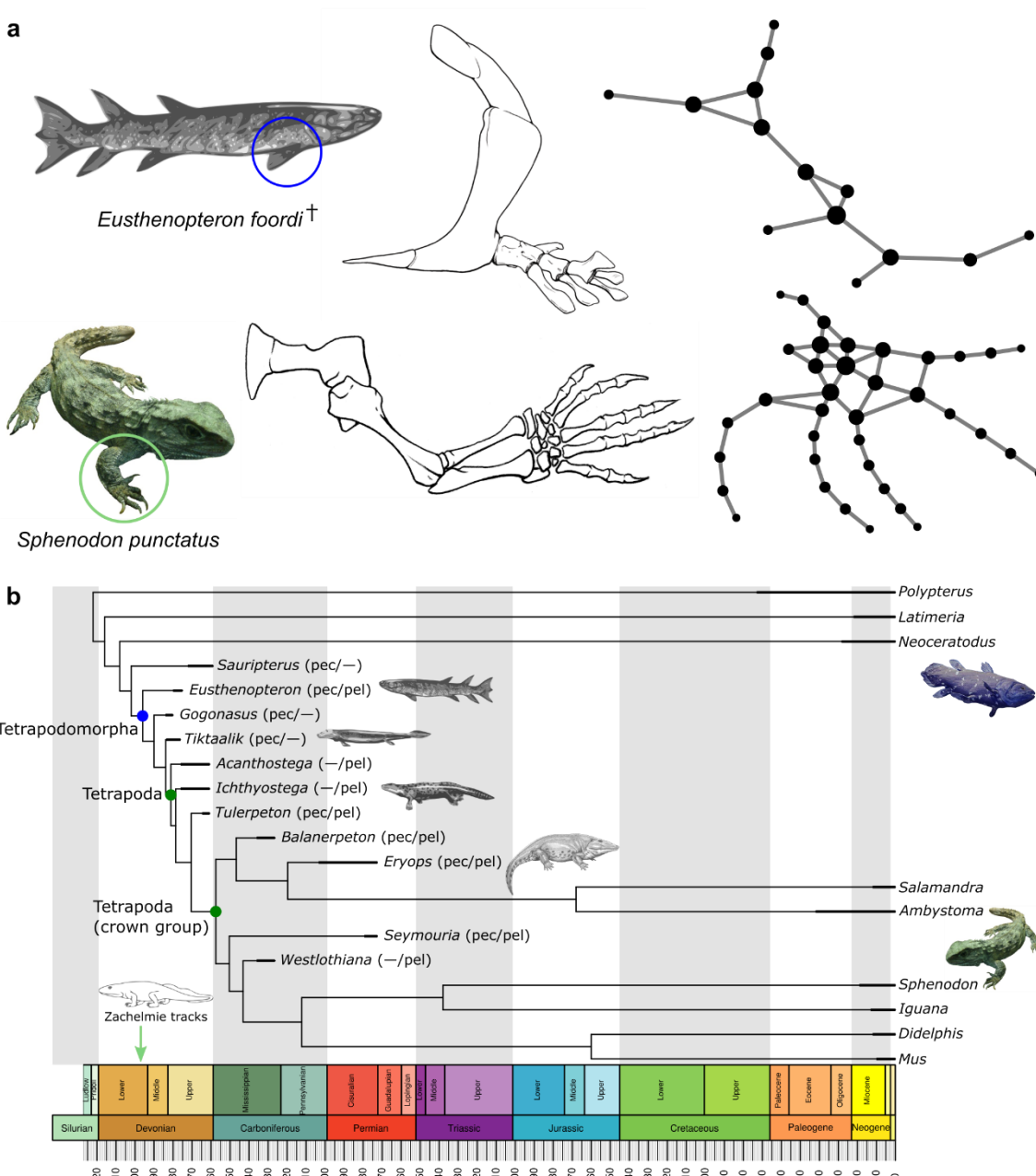
37 The evolution of tetrapod limbs from fish fins is heralded as one of the most important vertebrate
38 morphological and functional transitions^{1–8}. Establishing what makes an appendage a fin or a limb
39 is key to properly characterizing the fins-to-limbs transition³. Functional criteria are of limited use
40 because of the general consensus that limbs first evolved to move under water^{5,9}. Developmental
41 and palaeontological studies place the distinction between fins and limbs in the most distal region,
42 which bears the carpals/tarsals and digits in limbs and the radials and dermal lepidotrichia in fins^{3,10}.
43 The distinction between fins and limbs blurs when we look at the lobe-fins of transitional
44 tetrapodomorphs, such as *Eusthenopteron*, *Gogonasus*, and *Tiktaalik*^{11–13}. Both lobe-fins and limbs
45 share a division of the appendicular skeleton into three endoskeletal domains¹⁴, of which the most
46 distal one shows the greatest differentiation between sarcopterygian fishes (i.e., multi-patterned
47 radial bones) and tetrapods (i.e., autopod with a mesopod and digits). Although in the past,
48 researchers have disagreed about whether a zeugopod-mesopod boundary (wrist/ankle)^{15,16} or the
49 presence of digits alone³ is sufficient to define limbs, the current general convention is to define
50 “true” limbs as appendages with digits⁶. Even though the anatomical organization/topology of the
51 distal radials and the autopod superficially look similar (i.e., a series of skeletal elements joined
52 proximodistally)^{3,17} and they share a common genetic control or “deep homology”¹⁸, their
53 anatomical similarity has never been assessed quantitatively. Moreover, pectoral and pelvic lobe-
54 fins evolved into limbs in tandem during the fins-to-limbs transition, made possible due to the
55 recruitment of a common developmental genetic toolkit^{2,19}. Because pectoral and pelvic appendages
56 were originally different in their anatomy²⁰—and still are regarding the genetics of girdle
57 development²¹—we would expect to see a mix of evolutionary parallelisms/convergences
58 (homoplasy) and divergences, as shared and specific developmental programs and biomechanical
59 functions intertwined with each other during the fins-to-limb transition. Such a mix might result
60 from compromises between these “evo-devo” and “evo-biomechanical” constraints.

61

62 As appendages evolved, the anatomical similarity between pectoral and pelvic appendages also
63 evolved. Various authors have proposed alternative bottlenecks during evolution for the pectoral-
64 pelvic similarity (reviewed in refs ^{7,22}); these evolutionary bottlenecks represent times when
65 pectoral and pelvic appendages showed a greater anatomical similarity to each other (i.e., their
66 morphologies showed less disparity). Based on skeletal and muscular anatomical and
67 developmental features^{20,23–25}, pectoral-pelvic similarity bottlenecks have been proposed for the
68 origins of ray-finned fishes, coelacanths, tetrapodomorphs, and tetrapods. In a recent study
69 comparing the musculoskeletal network-anatomy of whole appendages²², we found evidence for a
70 pectoral-pelvic similarity bottleneck at the origin of sarcopterygians (as proposed by refs ^{3,7,20,25});

71 but not at the origin of tetrapods (as these same studies proposed). However, our previous work
72 focused only on the network-anatomy of extant taxa²². To further test the presence of a pectoral-
73 pelvic similarity bottleneck at the origin of tetrapods for the network-anatomy of the skeleton, we
74 have analysed a broader sample of extinct sarcopterygian fishes and early tetrapods across the fins-
75 to-limbs transition, including *Sauripterus*, *Eusthenopteron*, *Gogonasus*, *Tiktaalik*, *Acanthostega*,
76 *Ichthyostega*, *Tulerpeton*, *Balanerpeton*, *Eryops*, *Seymouria*, and *Westlothiana*; for which the fully-
77 articulated pectoral and/or pelvic anatomy is reasonably well known. A prediction of the hypothesis
78 of a pectoral-pelvic similarity bottleneck at the origin of tetrapods is that taxa closer to the split of
79 Tetrapoda within sarcopterygians—where the bottleneck is—will have a greater pectoral-pelvic
80 similarity (or lower disparity) than taxa that are farther away from the bottleneck.

81
82 To compare the skeletal anatomy of appendages in extinct and extant forms across the fins-to-limbs
83 transition, and better characterize anatomical parallelism/convergence and divergence between
84 pectoral and pelvic appendages, we focused our analysis on their anatomical organization or
85 network-anatomy; that is, the topological arrangement/pattern of skeletal elements of fully-
86 articulated appendages (**Fig. 1a**). This level of abstraction allowed us to compare evolutionary
87 changes that are not amenable to quantification using other morphometric methods due to the large
88 disparity of forms and presence/absence of parts between pectoral and pelvic fins and limbs^{22,26,27}.
89 Furthermore, the abstraction retains biological meaning in that the contacts between skeletal
90 elements reflect potential direct developmental and biomechanical interactions; for example,
91 ontogenetic sequences of ossification or embryonic interaction, and joint reaction forces or ranges
92 of motion. Using a network-based approach^{22,28,29}, we modelled the skeleton of fully-articulated
93 appendages as networks, in which nodes code for bones and links code for physical contact in a
94 standardized resting pose. We compared the evolution of eight network-based topological variables
95 (see *Methods* for details) in a phylogenetic context (**Fig. 1b**) to test whether (1) there are topological
96 differences between fins and limbs and between pectoral and pelvic appendages, (2) pectoral and
97 pelvic anatomy followed convergent/parallel or divergent modes of evolution during the fins-to-
98 limbs transition, and (3) there was an evolutionary bottleneck in pectoral-pelvic similarity in
99 tetrapods. We tested these hypotheses by comparing the occupation of appendicular morphospace,
100 estimating shift of evolutionary regimes, describing the evolution of disparity through time, and
101 testing bottlenecks with phylogenetic regressions.



102

103 **Figure 1. Network abstraction and phylogenetic context of the study. a**, Representative network
104 models of the skeletal anatomy of a fin and a limb; network nodes represent the bones of the
105 appendage and the links connecting them represent their physical articulations or joints. Note that
106 anatomical-network models are purely topological; thus, information about the size, shape, and
107 positioning of bones is not part of the model. Node size is drawn proportional to the bone's number
108 of articulations. **b**, Time calibrated phylogenetic tree assembled for this study showing which taxa
109 have complete information for pectoral and pelvic appendages: pec/pel, both appendages found in
110 articulation or completely reconstructed; —, complete appendage not preserved. Image of tetrapod
111 outline by Mateus Zica (GFDL), body fossil restorations by Nobu Tamura (CC BY-SA 3.0),
112 coelacanth by Zoo Firma (CC BY-SA 3.0), and tuatara by Tim Vickers (CC BY-SA 3.0).

113

114

115 **RESULTS**

116 **Topological Discrimination of Appendages**

117 The network-anatomy of the appendicular skeleton varied for each taxon and between pectoral and
118 pelvic regions (**Table 1**). We used a Principal Component Analysis (PCA) to visualize global
119 patterns of topological variance across anatomical networks and test for differences between fins
120 and limbs, pectoral and pelvic appendages, and extinct and extant species.

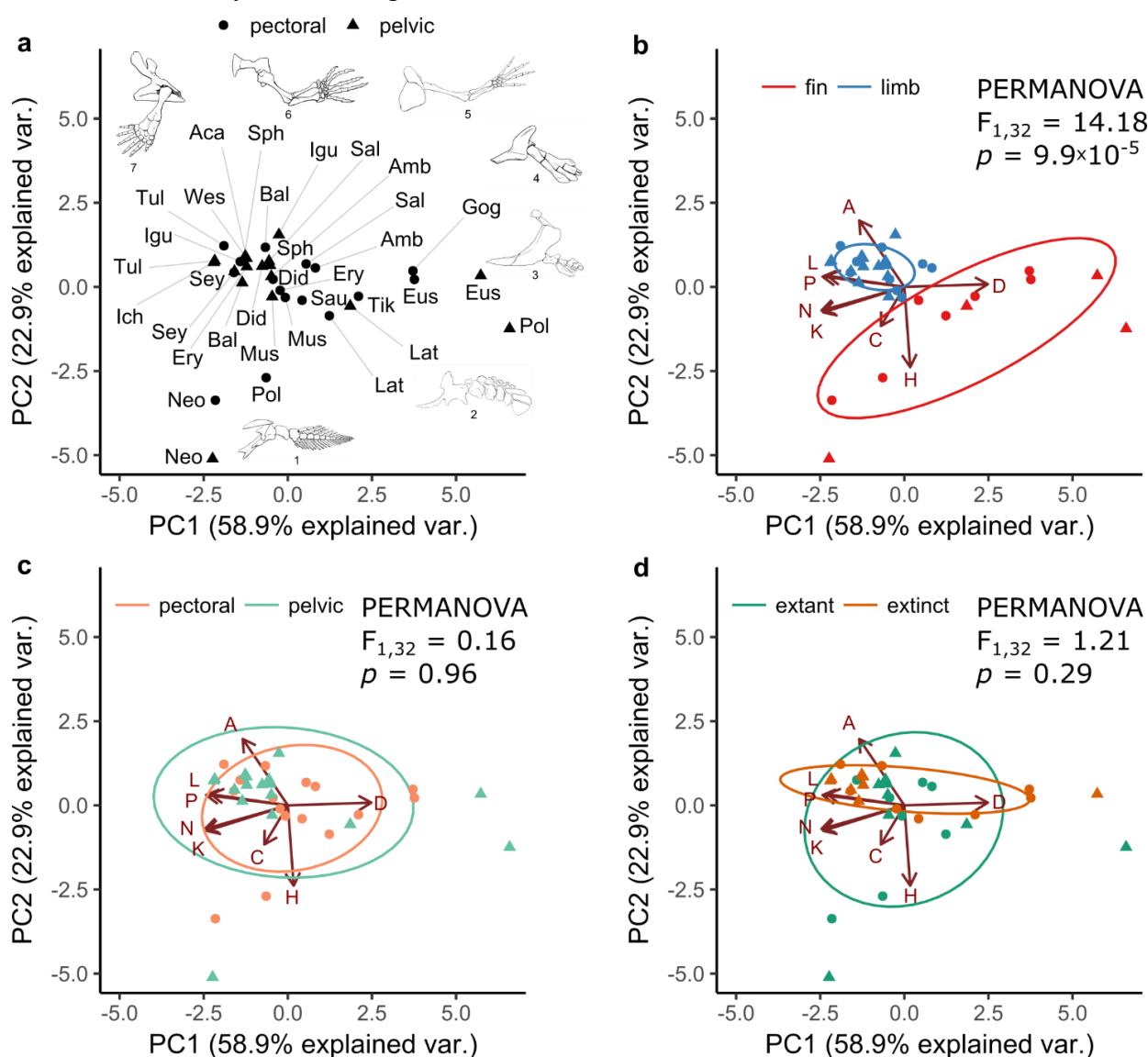
121

122 The first two PCA components explained 81.8% of the total topological variation among
123 appendages (**Fig. 2a**). The first axis of variation (58.9%) broadly discriminated between (i) more
124 modular (higher P) sparsely connected (lower D) appendages, such as limbs, and (ii) less modular
125 (lower P) densely packed (higher D) appendages, such as lobe-fins. The second axis of variation
126 (22.9%) broadly discriminated between (i) more regular appendages, in which bones tend to have
127 the same number of articulations (lower H) and which contact bones with a similar number of
128 articulations (high A), such as limbs and anatomically plesiomorphic lobe-fins, and (ii) more
129 heterogeneous appendages, in which bones have a varying number of articulations (higher H) and
130 which preferentially contact bones with a different number of articulations (lower A), such as in the
131 anatomically derived lobe-fins of *Neoceratodus*.

132

133 A permutational multivariate analysis of variance (PERMANOVA) showed a statistically significant
134 difference in topological variability between fins and limbs ($F_{1,32} = 14.18, p = 9.9 \times 10^{-5}$; **Fig. 2b**).
135 The assortativity of appendages (i.e., tendency of bones to contact bones with a similar number of
136 connections) was the main discriminator between fins and limbs, which occupied opposite positions
137 along the assortativity-axis of variation. Limbs had larger and positive values, whereas fins had
138 lower and negative values. We can explain this difference by the presence of the autopod in limbs
139 and, more specifically, by the presence of digits. Phalanges and, to a lesser extent, carpal/tarsal
140 bones, tend to articulate with other autopodial bones with a similar number of articulations. For
141 example, phalanges connect in a proximodistal series to other phalanges or metacarpals/metatarsals,
142 so that most phalanges have two articulations (one proximal one distal) to other phalanges that also
143 have two articulations (hence A increases). A similar pattern may occur among carpal/tarsal bones
144 because of their nearly-polygonal shapes. PERMANOVA showed no significant difference in
145 topological variability between pectoral and pelvic appendages ($F_{1,32} = 0.16, p = 0.96$; **Fig. 2c**) and
146 between extinct and extant species ($F_{1,32} = 1.21, p = 0.29$; **Fig. 2d**). Pectoral and pelvic appendages
147 did not occupy different areas of the morphospace, which indicates that they share a similar
148 topological organization. Although extinct and extant taxa are statistically indistinguishable, they
149 appear to occupy slightly different areas of morphospace differently: extant species varied equally

150 along PC1 and PC2 axes, while the variance in extinct species is primarily concentrated along the
 151 PC1 axis and barely varied along the PC2 axis.



152
 153 **Figure 2. Biplots of the first two PCA components of topological variables for pectoral**
 154 **(circles) and pelvic (triangles) appendages combined.** **a,** Distribution of pectoral and pelvic
 155 appendages for each taxon in the sample (abbreviated by the first three letters of the genera).
 156 For reference we included line drawings representing different appendages: (1) *Neoceratodus*
 157 pectoral, (2) *Latimeria* pelvic, (3) *Eusthenopteron* pelvic, (4) *Gogonasus* pectoral, (5) *Salamandra*
 158 pectoral, (6) *Acanthostega* pelvic, and (7) *Sphenodon* pectoral. **b,** Comparison of limbs vs. fins (i.e.,
 159 appendages with and without digits, respectively) showed that they occupy different regions of the
 160 morphospace. **c,** Comparison of pectoral vs. pelvic appendages showed that they occupy
 161 overlapping regions of the morphospace. **d,** Comparison of extant vs. extinct taxa showed that they
 162 occupy the PC2 axis in different ways. Red arrows show the contribution to the first two PCA
 163 components of each network variable: (N) nodes, (K) links, (D) density, (C) clustering coefficient,
 164 (L) path length, (H) heterogeneity, (A) assortativity, and (P) parcellation.

165

166 Evolution of Pectoral and Pelvic Appendages

167 We assessed the potential for parallel/convergent and divergent changes in topology for pectoral and
168 pelvic appendages by estimating shifts in evolutionary regimes (SURFACE) and analysing disparity
169 through time (DTT).

170

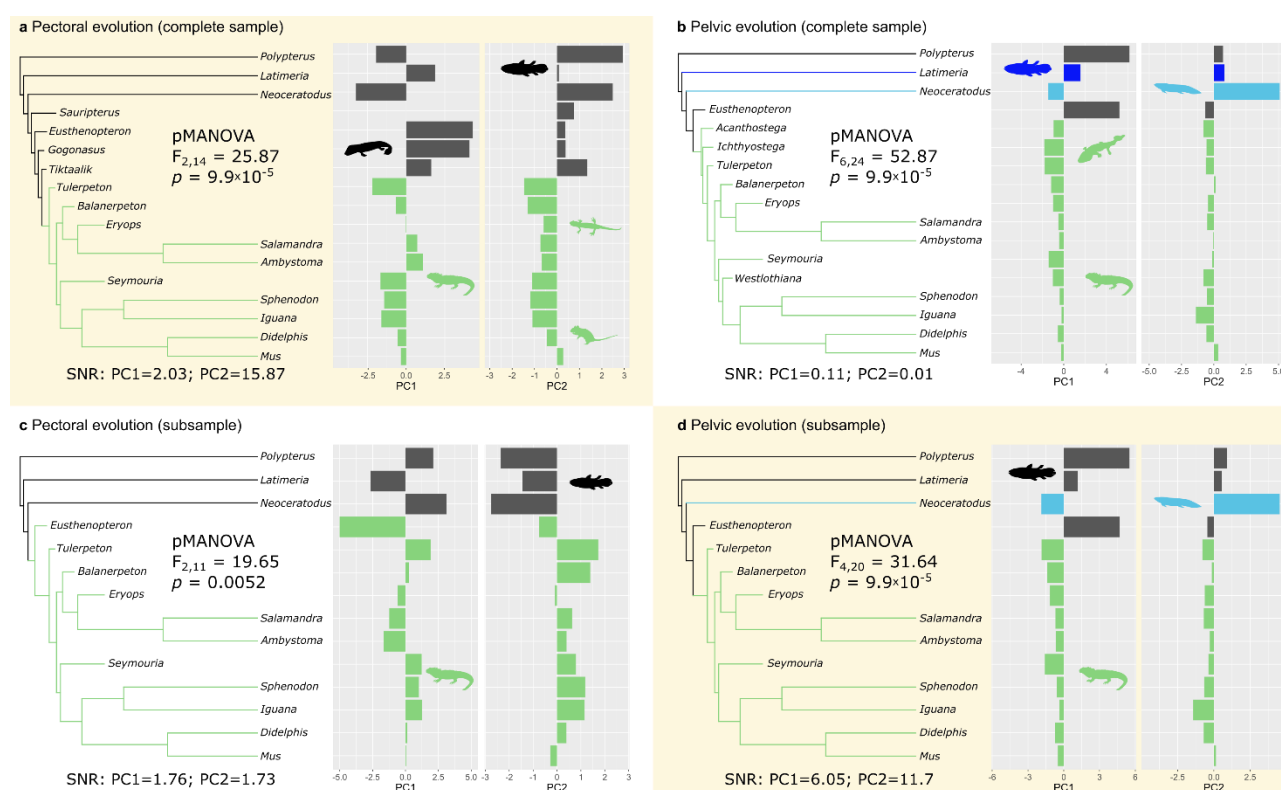
171 The SURFACE analysis on PC1 and PC2 estimated a shift in mean values at the root branch of
172 Tetrapoda for the complete sample of pectoral appendages (**Fig. 3a**); thus, dividing the sample into
173 two regimes, one for radial-bearing taxa and another for digit-bearing taxa. The signal-to-noise ratio
174 of this estimated pattern was higher than one (PC1 = 2.03; PC2 = 15.87), which indicates a high
175 effect size of both variables in discriminating groups and adequate power to detect shifts.

176 Comparisons of alternative evolutionary models using AIC weights showed that an Ornstein-
177 Uhlenbeck model with multiple rates of change (sigma) and optimal means (theta) best explains the
178 evolution of pectoral appendages (**Supplementary Table 1**). A phylogenetic MANOVA confirmed
179 a statistically significant difference between pectoral fins and pectoral limbs ($F_{1,32} = 25.87, p =$
180 9.9×10^{-5}). A similar pattern was found when we analysed only those taxa for which we had a pelvic
181 correspondence in the sample. In this pectoral subsample, the estimated new regime also included
182 *Eusthenopteron* (**Fig. 3b**), which placed the shift in mean values at the root branch of
183 Tetrapodomorpha (rather than Tetrapoda). The signal-to-noise ratio for the pectoral subsample was
184 above one (PC1 = 1.76; PC2 = 1.73); enough to detect a difference, but weaker than for the
185 complete sample. Likewise, an Ornstein-Uhlenbeck model was the best fit and phylogenetic
186 MANOVA showed a statistically significant difference between the two groups, both including
187 *Eusthenopteron* ($F_{2,11} = 19.65, p = 0.0052$) and excluding it ($F_{2,11} = 20.2, p = 6.9 \times 10^{-4}$). The
188 congruence of results added support to the estimated shift in topological organization during the
189 fins-to-limbs transition.

190

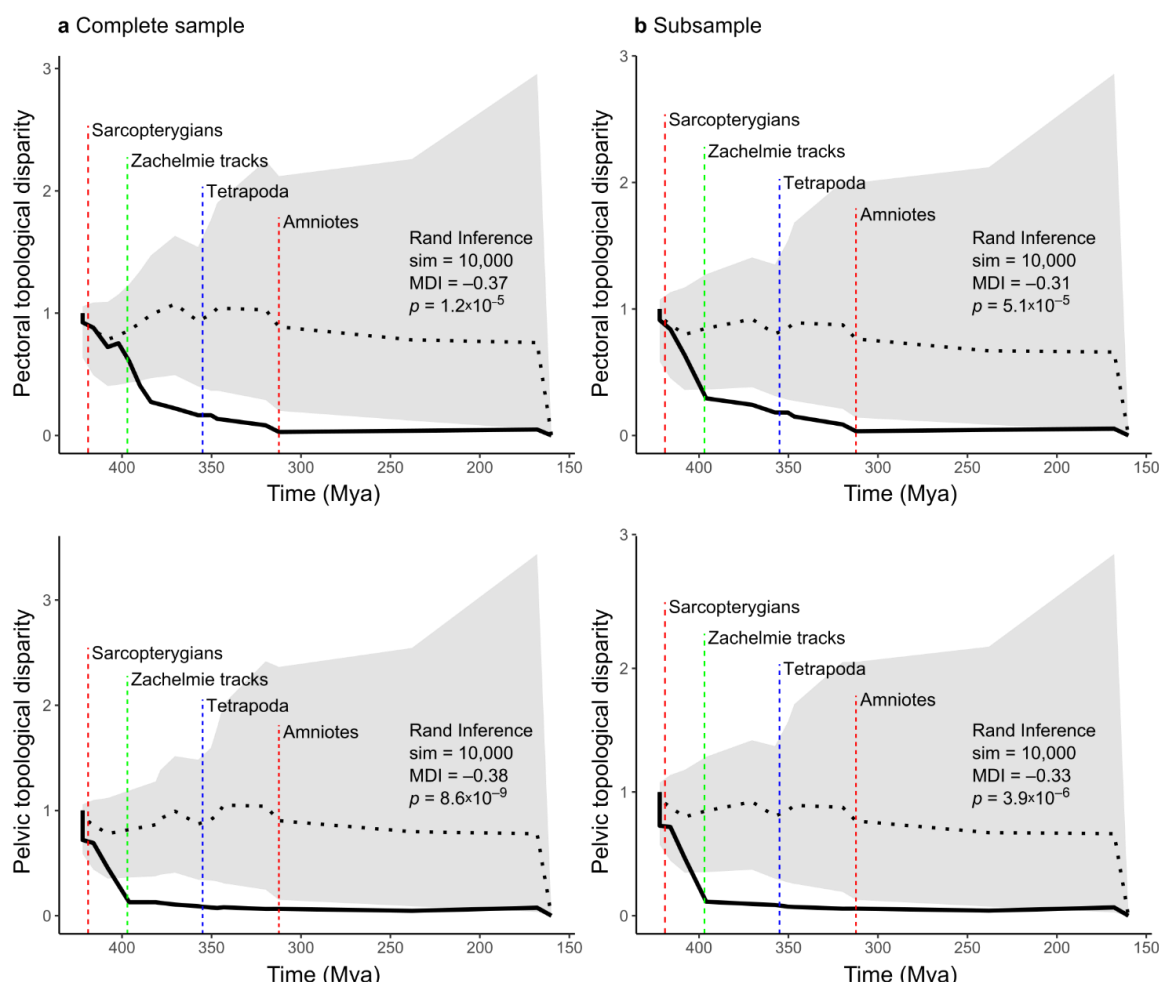
191 The SURFACE analysis for the complete sample of pelvic appendages estimated three shifts of
192 mean values (**Fig. 3c**): one at the root branch of Tetrapoda, and another two in the lineage of
193 *Latimeria* and *Neoceratodus*. However, the signal-to-noise ratio of the estimated pattern was below
194 one for both variables (PC1 = 0.11; PC2 = 0.01), which indicated a lack of effect size and power to
195 discriminate between groups. Comparisons of alternative models using AIC weights showed that an
196 Ornstein-Uhlenbeck model with multiple optimal means (theta) better fitted the evolution of pelvic
197 appendages (**Supplementary Table 1**). Despite the low signal-to-noise ratio, phylogenetic
198 MANOVA confirmed a statistically significant difference between radial-bearing taxa vs. digit-
199 bearing taxa ($F_{2,14} = 47.17, p = 9.9 \times 10^{-5}$). A similar pattern was found when we analysed only those

200 taxa for which we have a pectoral correspondence in the sample. In this pelvic subsample, only two
 201 shifts were estimated: one at the root branch of Tetrapoda and another in the lineage of
 202 *Neoceratodus* (**Fig. 3d**). In contrast to what happened for the complete sample of pectoral
 203 appendages, these regime shifts had a signal-to-noise ratio higher than one for both variables (PC1
 204 = 6.05; PC2 = 11.7). Like for the complete sample, an Ornstein-Uhlenbeck model was the best fit
 205 and a phylogenetic MANOVA showed a statistically significant difference between radial-bearing
 206 taxa and digit-bearing taxa ($F_{2,11} = 34.72, p = 0002$).



207
 208 **Figure 3. Estimated evolutionary shifts using SURFACE.** **a**, Estimation using the complete
 209 sample of pectoral appendages. **b**, Estimation using the subsample of pectoral appendages having
 210 both appendages represented in the sample. **c**, Estimation using the complete sample of pelvic
 211 appendages. **d**, Estimation using the subsample of pelvic appendages having both appendages
 212 represented in the sample. Both appendages showed a regime shift in Tetrapoda, indicated in green.
 213 Other single-lineage shifts found in lobe-finned fishes were highlighted in shades of blue. Yellow
 214 background marks SURFACE tests with a signal-to-noise ratio (SNR) above one. Significant SNR
 215 indicated evolutionary shifts at the origin of digit-bearing taxa for both pectoral and pelvic
 216 appendages, with a potential independent shift in *Neoceratodus* pelvic fin evolution. Evolutionary
 217 shifts toward different topologies were validated by phylogenetic MANOVA tests.
 218
 219 Topological disparity decreased through time for pectoral and pelvic appendages alike (**Fig. 4a**;
 220 *solid black line*). DTT tests for the complete samples showed a statistically significant decrease of
 221 disparity in pectoral (MDI = -0.37, $p = 1.2 \times 10^{-5}$) and pelvic appendages (MDI = -0.38, $p = 8.6 \times 10^{-5}$)

222 9) in the timespan between the origins of sarcopterygians and amniotes (**Fig. 4a; red dashed lines**).
 223 For pectoral appendages, the decay was more exponential between sarcopterygians and amniotes.
 224 For pelvic appendages, there was a pronounced linear decay until a turning point that was roughly
 225 concurrent with the age of the oldest purported tetrapod tracks (**Fig. 4a; green dashed line**); after
 226 that point disparity continued mostly steady through time. As the pelvic appendage dataset contains
 227 few tetrapodomorph fish, we subsampled the two datasets to contain similar taxonomic spread. The
 228 subsampled DTT showed similar patterns between pectoral and pelvic appendages, with a change in
 229 disparity coincident with the age of the oldest tetrapod tracks (**Fig. 4b**). This match indicates that
 230 removal of tetrapodomorphs fishes (*Sauripterus*, *Gogonasus*, and *Tiktaalik*) reduced the disparity of
 231 appendages in the time-frame of interest.

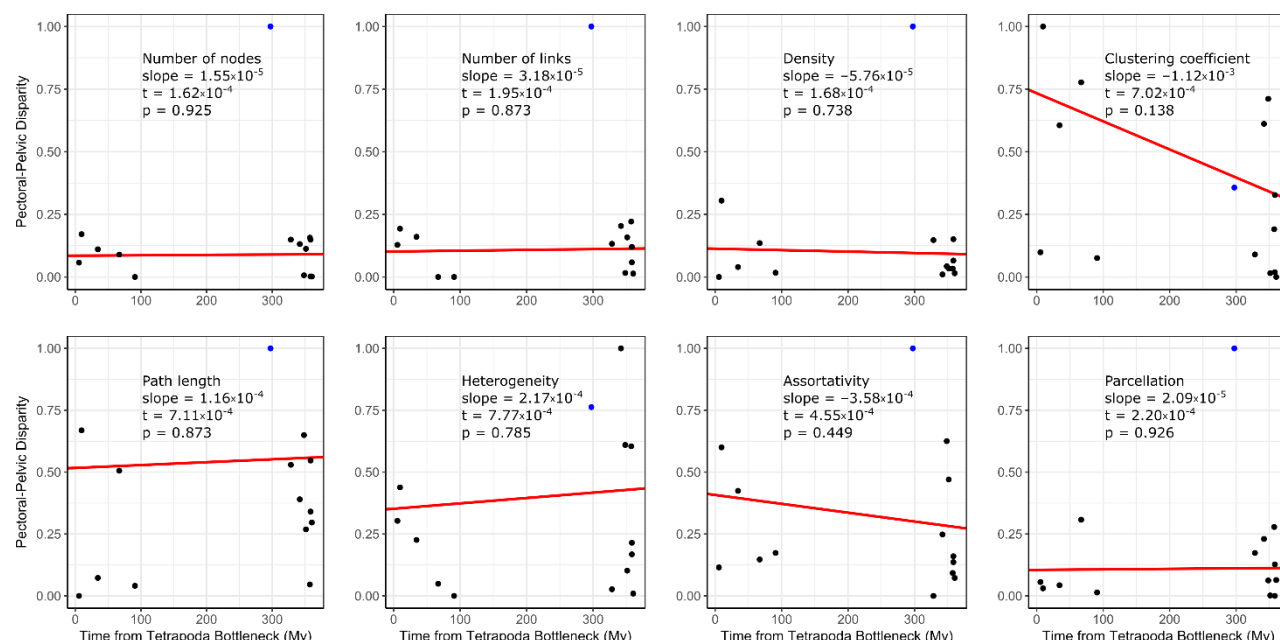


232
 233 **Figure 4. Topological disparity through time for pectoral and pelvic appendages.** **a**, Complete
 234 samples. **b**, Subsamples with only taxa having both appendages modelled. There was a decay in
 235 disparity (*solid black line*) for both appendages, which varied in the rate of decay in different
 236 periods of time. Grey areas show the 95% CIs of the expected disparity based on 10,000
 237 phylogenetic simulations under Brownian motion. Horizontal black dotted line shows the mean of
 238 disparity for all simulations. Vertical colour dashed lines mark key events (e.g., divergence times) in
 239 sarcopterygian evolution for reference.

240

241 **Pectoral-Pelvic Similarity Bottleneck**

242 To test the similarity bottleneck hypothesis, we performed a phylogenetic generalized least square
243 (PGLS) regressions of pectoral-pelvic disparity against time from Tetrapoda, for each of the
244 topological variables. As a proxy for similarity we used disparity, calculated as the absolute residual
245 of pectoral and pelvic network variables to the identity line (lower disparity = higher similarity).
246 The bottleneck hypothesis predicts regression slopes significantly greater than zero for disparity
247 against time. Because the bottleneck marks the point of minimum disparity (maximum similarity),
248 taxa far from the bottleneck would have higher disparity (lower similarity) than taxa close to the
249 bottleneck. None of the PGLS regressions were statistically significant (Fig. 5), which means that
250 the topological arrangement of the pectoral-pelvic appendages does not support a similarity
251 bottleneck at the origin of Tetrapoda.



252

253 **Figure 5. Testing the pectoral-pelvic similarity bottleneck hypothesis for Tetrapoda.** PGLS
254 regression slopes (in red) were not different from zero in any of the eight variables analysed; thus,
255 rejecting the presence of a pectoral-pelvic similarity bottleneck for the topological organization of
256 the appendicular skeleton. A significantly positive slope would be consistent with a bottleneck. Blue
257 dot marks the ray-finned fish *Polypterus*, which behaves as an outlier in some comparisons.

258

259 **Alternative Anatomical Interpretations**

260 In building anatomical networks of appendicular skeletons, we included only bones and
261 articulations whose presence we were confident about (“minimal networks”). However, 11 of the 34
262 appendages modelled had one or more articulations for which we were uncertain about their
263 presence; mostly involving mediolateral contacts between bones in extinct taxa. We accounted for

264 variations due to the presence/absence of these articulations by analysing network models that also
265 included these uncertain articulations (“extended networks”). Regardless of minor changes in the
266 values of some topological variables, the main results and interpretation for extended networks were
267 the same as for minimal networks (see details in **Supplementary Results**). This indicated that our
268 analysis could accommodate informed variations in network models, due to alternative
269 interpretations of the anatomy of appendages, without nullifying the main results and conclusions of
270 this study.

271

272

273 **DISCUSSION**

274 The evolution of tetrapod limbs from fish fins occurred through a series of anatomical changes,
275 including the loss/gain of girdle elements, acquisition of wrist/ankle joints, and the development of
276 digits⁵. Here we demonstrated that digits had the greatest impact on the evolution of the anatomy of
277 the appendicular skeleton. Topological variables discriminated between digit-bearing taxa and
278 radial-bearing taxa, which occupied distinct regions of the morphospace (**Fig. 2**). Studies based on
279 different appendicular skeletal traits also discriminated between digit-bearing taxa and radial-
280 bearing taxa³⁰. From a topological viewpoint, digits increased the number of bones (N) and
281 articulations (K) of appendages, but in such a way (in contrast to carpal/tarsal topological
282 arrangement of bones) that both the relative density of articulations (D) and the heterogeneity of
283 number of articulations of bones (H) decreased. At the same time, phalanges articulating one-on-
284 one proximodistally increased the overall path length (L) of appendages and the assortativity of
285 bones (A). Finally, the formation of new digit modules increased the parcellation (P) of limbs
286 compared to lobe-fins, making them more modular²². The origin of digits was concomitant with the
287 parallel evolution of pectoral and pelvic limbs toward a region of the morphospace (**Fig. 2a**, top-
288 right) where digit-related features predominated (high N, K, A, P; low D, H). Our results also
289 showed a significant evolutionary shift in the topological anatomy for digit-bearing taxa (**Fig. 3**)
290 that departed from the previous evolutionary regime observed in radial-bearing taxa, even in
291 intermediate forms such as *Eusthenopteron*, *Gogonasus*, and *Tiktaalik*. These findings are not a
292 surprise if one acknowledges the presence of digits as a morphological and evolutionary
293 novelty^{26,31-33}, regardless of shared developmental histories or “deep-homologies” between digits
294 and radials³⁴⁻³⁸. Novelties that increase the potential morphological morphospace provide an
295 opportunity for greater diversification³⁹. The evolutionary separation of digit-bearing taxa in the
296 morphospace and in evolutionary estimations is in line with the idea of limbs as having evolved a
297 truly novel anatomical reorganization⁴⁰. This novelty has well-recognized functional implications
298 for the origin of terrestrial locomotion, but the evidence for modularity may have more than

299 developmental implications. By partitioning fins into more modular limbs there should have been
300 more potential for localized functional specializations of bones, joints, muscles and more; including
301 differential functions of pectoral and pelvic appendages⁹. Such potential would also arise from the
302 modified degrees of freedom of the limb, transformed from somewhat homogeneous, flexible fins
303 into fewer, more stiffened distal limb joints (i.e. in the autopodium). This is a logical speculation
304 even though our analysis of bone topological networks is unable to account for details of the
305 lepidotrichia.

306

307 The topological disparity of pectoral and pelvic appendages also decreased during the timespan
308 between the origin of sarcopterygians and the origin of amniotes (**Fig. 4a**). A divergent pattern was
309 observed for pectoral and pelvic appendages, when we considered all appendages studied (i.e., the
310 complete sample). Whereas pectoral disparity decreased exponentially within this time interval,
311 pelvic disparity only decreased linearly, until approximately the time of the earliest described
312 tetrapod trackways (e.g., the Zachełmie tracks from the Middle Devonian⁴¹; similar in timing to
313 other records pre-dating substantial body fossils^{42,43}) and then it stabilized. This pattern, although
314 based on a modest sample size as mandated by the existing fossil record, is congruent with an
315 evolutionary stabilization of the disparity of pelvic anatomical organization near the origin of
316 tetrapods, which did not occur for pectoral appendages until deeper within the tetrapod stem
317 lineage. It is possible that this pattern is a result of few tetrapodomorph fish in our sample; when
318 *Sauripterus*, *Gogonasus*, and *Tiktaalik* were removed from the pectoral analysis, we got the same
319 pattern as for the pelvis. When the same taxa are included in the analyses, topological disparity
320 decreased in parallel for pectoral and pelvic appendages, with both showing a shift in the decay rate
321 coincident with the Zachełmie (and, approximately, other) tracks (**Fig. 4b**). If we consider these
322 earliest tetrapod trackways part of the fins-to-limbs transition, our results would suggest that the
323 transition indirectly decreased the morphological variation, which may have constrained the
324 evolution of different topologies in limbs (see, for example, the morphospace occupation of limbs in
325 **Fig. 2c**). This would agree with a dynamic compromise between possibly different functional
326 demands in pectoral and pelvic appendages during the water-to-land transition⁹ and a shared
327 developmental program constraining the evolvability of limbs⁴⁴ (constraints that are still strong
328 even in more deeply nested tetrapod lineages like primates⁴⁵). Differing constraints and perhaps
329 compromises have also been proposed to explain a decrease of disparity in the lower jaw of
330 tetrapodomorphs across the water-to-land transition⁴⁶. However, while functional trade-offs are
331 likely for the feeding vs. locomotor systems of stem tetrapods, this de-coupling remains to be
332 studied for the craniocervical region, which was likely more constrained in tetrapodomorphs by
333 mechanical interactions between the pectoral appendage, axial column, and skull.

334

335 Previous studies have suggested the presence of bottlenecks in pectoral-pelvic anatomical similarity
336 during the evolution of vertebrates^{7,20,23–25}. One similarity bottleneck was proposed at the origin of
337 tetrapods coincident with the fins-to-limbs transition^{7,25}. This bottleneck was supported by data
338 from general morphological features (e.g., shape and size similarities, presence/absence of
339 homologous bones)³ and overall configuration and number of muscles²⁵. Our disparity *vs.* time
340 regression tests (**Fig. 5**) rejected the presence of this bottleneck for the eight topological variables
341 measured for taxa across the fins-to-limbs transition. These new tests override our previous
342 tentative support for this bottleneck from the analysis of the network-anatomy of extant taxa
343 alone²². Our result, based on the network-anatomy or topological organization of the skeleton,
344 differs of previous observations based on different skeletal and muscular features. One possible
345 resolution to this apparent contradiction is that bones and muscles may have had a de-coupled
346 evolution during the fins-to-limbs transition, mirroring the idea that bones and muscles can respond
347 differentially in time and magnitude to evolutionary pressures^{47–49}. Lingering challenges for this
348 question include the differing nature of data in bottleneck analyses (e.g. phylogenetic characters³;
349 muscular attachments²⁵) relative to this study, in addition to other complex traits not yet considered
350 in such analyses, such as lepidotrichia.

351

352 Our study of the network-anatomy of appendages during the fins-to-limbs transition revealed an
353 overall parallelism in the evolution of pectoral and pelvic appendages during this time, shaped
354 greatly by the origin of digits. Digits were a morphological novelty that significantly changed the
355 topological features of appendages, clearly discriminating limbs from fins and even from
356 transitional forms. The presence of digits produced a directional evolutionary shift towards
357 appendages that overall were less densely and heterogeneously connected, but more assortative and
358 modular. Digits evolved in the context of a general decrease in topological disparity among pectoral
359 as well as pelvic appendages, which may have had an impact on the subsequent evolution of
360 tetrapods in terms of function, behaviour, and ecology.

361

362

363 METHODS

364 **Anatomy of extinct taxa.** We examined the skeletal anatomy of the pectoral and pelvic appendages
365 in 11 extinct taxa: *Sauripterus taylory* Hall 1843; *Eusthenopteron foordi* Whiteaves 1881;
366 *Gogonasus andrewsae* Long 1985; *Tiktaalik roseae* Daeschler, Shubin & Jenkins, 2006;
367 *Acanthostega gunnari* Jarvik 1952; *Ichthyostega* sp. Säve-Söderbergh 1932; *Tulerpeton curtum*
368 Lebedev 1984; *Balanerpeton woodi* Milner & Sequeira 1994; *Eryops megacephalus* Cope 1877;

369 *Seymouria baylorensis* Broili 1904; and *Westlothiana lizziae* Smithson and Rolfe 1990. Our
370 resources included museum collections, photographs and literature descriptions (see details in
371 **Supplementary Materials**). These taxa were selected because they have articulated specimens with
372 complete pectoral and/or pelvic appendages for examination and/or described in the literature. We
373 only considered incomplete or disarticulated materials when a full, rigorous reconstruction of the
374 appendage was available in the literature. Finally, we decided to exclude from the analysis those
375 appendages for which the complete skeletal anatomy could not be confidently reconstructed due to
376 a large number of missing elements, namely: pectoral appendages of *Acanthostega*, *Ichthyostega*,
377 and *Westlothiana*; and pelvic appendages of *Sauripterus*, *Gogonasus*, and *Tiktaalik*.
378

379 **Anatomy of extant taxa.** We examined the skeletal anatomy of pectoral and pelvic appendages in
380 nine extant taxa. Six of them were recently described elsewhere²²: *Polypterus senegalus* Cuvier
381 1829; *Latimeria chalumnae* Smith 1939; *Neoceratodus forsteri* Krefft 1870; *Ambystoma*
382 *mexicanum* Shaw 1789; *Salamandra salamandra* Linnaeus 1758; and *Sphenodon punctatus* Gray
383 1842. In addition, we built network models for *Iguana iguana* Linnaeus 1758; *Didelphis virginiana*
384 Kerr 1792; and *Mus musculus* Linnaeus 1758 (see details in **Supplementary Materials**). We
385 selected these extant taxa because there were available dissection data and because they bracket the
386 fins-to-limbs transition (i.e., rootward and crownward relative to Tetrapoda/Amniote).
387

388 **Network modelling.** We built unweighted, undirected network models for the appendicular
389 skeleton, where nodes coded for bones and links connecting nodes coded for physical articulation or
390 contacts between two bones. Network models included the girdle and fin/limb skeleton. For the
391 girdles, we considered all skeletal elements present or presumed as present: in pectoral girdles,
392 these may include interclavicle, clavicle, supracleithrum, anocleithrum, cleithrum, and
393 scapulocoracoid; in pelvic girdles these may include the hip bones fused (pelvis) or divided into two
394 or three parts (ilium, pubis, and ischium). For fin and limb skeletons we considered all
395 endochondral elements with a sufficient degree of ossification to be directly observed, as well as
396 those elements for which there was enough indirect evidence (for example, an articular surface in
397 another bone). We decided to exclude peripheral dermal elements, such as lepidotrichia and scales,
398 from the fin network models for two main reasons. Firstly, it is often impossible to precisely
399 identify their physical contacts to other elements in fossil taxa; secondly, their absence in digit-
400 bearing taxa adds noise to the comparison of the skeletal topology between fins and limbs using
401 network analysis.
402

403 We coded the articulations among bones following detailed descriptions of each taxon (see
404 **Supplementary Materials**). When in doubt, we considered physical contiguity and adjacency as
405 presence of articulation, which allowed us to code for contacts between bones in fossils that did not
406 preserve details of the articular surface due to lack of preservation. Nevertheless, it was sometimes
407 difficult to discern the presence/absence of a given contact between two bones in fossil taxa. We
408 tackled this uncertainty at the modelling level and at the analysis level. At the modelling level, by
409 building two types of networks for each appendage: a minimal network that includes the contacts
410 with high certainty and an extended network that includes also potential, but more uncertain
411 contacts (see **Supplementary Materials**). This assesses whether different criteria may affect the
412 evolutionary patterns reported. At the analysis level, by performing a robustness tests of network
413 parameter values under the assumption of random noise or sampling error (see below).

414

415 **Anatomical network analysis.** We characterized the architecture of fins and limbs using eight
416 topological variables (network parameters): number of nodes (N) and number of links (K), density
417 of connections (D), mean clustering coefficient (C), mean path length (L), heterogeneity of
418 connections (H), assortativity of connections (A), and parcellation (P). In short, parameters N and K
419 are counts of the number of bones and physical contacts among bones, respectively. D measures the
420 actual number of connections divided by the maximum number possible (it ranges from 0 to 1); D
421 increases as new bones evolve if they form many new articulations, otherwise it decreases. C
422 measures the average of the ratio of a node's neighbours that connect among them (it ranges from 0
423 to 1); in the appendicular skeleton, triangular motifs can form by adding mediolateral articulations
424 to the most commonly present proximodistal ones. L measures the average number of links required
425 to travel between two nodes (minimum 1); L will increase, for example, by the presence of serial
426 bones articulating one-on-one proximodistally. H measures the variability in the number of
427 connections of nodes as the ratio between the standard deviation and the mean of the number of
428 connections of all nodes in the network (minimum 0); appendages where each bone has a different
429 number of articulations will have a high H, while if bones have the same number of articulations
430 (i.e., forming a regular pattern) the appendage will have a low H. A quantifies the extent to which
431 nodes with the same number of connections connect to each other (positive if nodes with the same
432 number of connections connect to each other, negative otherwise); when this happens A is positive,
433 whereas the inverse tendency means that A is negative. Finally, P measures the degree of modularity
434 of the network (it ranges from 0 to 1); appendages with more network-modules and with bones
435 evenly distributed among modules will have a high P. See the **Supplementary Materials** for further
436 mathematical details. We measured topological variables in R⁵⁰ using functions from the package
437 *igraph*⁵¹.

438

439 **Parameter robustness.** We tested the robustness of topological variables to potential errors in
440 assessing the presence of bones and articulations by comparing the observed values to a randomly
441 generated sample of 10,000 noisy networks for each anatomical network. We created noisy
442 networks by randomly rewiring the links of the original network with a 0.05 probability, which
443 results in introducing a 5% artificially generated error. Then, we compared the observed values of
444 empirical networks to the sample of noisy networks. In each case, we tested the null hypothesis that
445 observed values are equal to the sample mean. We rejected the null hypothesis with $\alpha = 0.05$ if the
446 observed value is in the 5% end of the distribution of simulated values (**Supplementary Table 2**;
447 “TRUE”, cannot reject H_0 ; “FALSE”, reject H_0 with $\alpha = 0.05$). We tested a total of 272 values (34
448 networks x 8 parameters): 268 fell within the confidence intervals and scored “TRUE” in the test.
449 The exceptions were for *Neoceratodus* pectoral path length, *Neoceratodus* pelvic clustering
450 coefficient and path length, and *Didelphis* pelvic parcellation. Because the anatomy of
451 *Neoceratodus* and *Didelphis* derived from our own dissections, these few cases of rejection of the
452 null hypothesis for these parameters can be attributed to the difficulty for a random-noise process to
453 produce realistic dissection errors (for example, by coding the femur as not articulating with the
454 pelvis).

455

456 **Phylogenetic relationships.** We assembled a phylogenetic tree for our study taxa according to the
457 approximate majority view in published phylogenies^{52–54}. We calibrated the tree branches using the
458 ‘equal’ method defined by Lloyd^{55,56} to adjust zero-length and internal branches, as implemented in
459 the package *paleotree*⁵⁷ for R. Temporal ranges of taxa (first and last appearance date in Ma) follow
460 those of the Paleobiological Database (www.paleodb.org) and TimeTree (www.timetree.org)
461 (**Supplementary Tables 4 and 5**). We constrained tree calibration by assigning minimum dates for
462 known internal nodes (clades or splits) based on molecular inferences and fossil dates from the
463 literature (*op. cit.*). The exact dates for first and last appearance of taxa and for internal nodes are
464 available within source code attached. Note that when required by the analysis, the main tree was
465 pruned to only include those taxa of interest.

466

467 **Analysis of topological variation.** We ran a principal component analysis (PCA) of topological
468 variables by a singular value decomposition of the centred and scaled measures using the function
469 *prcomp* in the R build-in package *stats*⁵⁰. We used PCA components to test whether the anatomical
470 organization of the appendicular skeleton differed (1) between fins (without digits) and limbs (with
471 digits), (2) between pectoral and pelvic appendages, and (3) between extinct and extant taxa. We
472 performed a permutational multivariate analysis of variance (PERMANOVA) over 10,000

473 permutations using the function *adonis* in the R package *vegan*⁵⁸. PERMANOVA used a
474 permutation test with pseudo-F ratios on the Euclidean distances of the matrix of PCA components
475 to test the null hypothesis that the centroids and dispersion were equivalent for each group
476 comparison. Rejection of the null hypothesis meant that the network topology differed between the
477 groups compared.

478

479 **Evolutionary modelling.** We estimated the occurrence of evolutionary shifts in the topological
480 organization of appendages in our phylogenetic tree using a SURFACE⁵⁹ analysis of the first two
481 PC components for pectoral and pelvic appendages, independently. SURFACE estimates change of
482 evolutionary regimes—in the strength (α) and rate (σ) of evolution and in the optimal mean (θ)—
483 from multivariate data and a non-ultrametric tree. SURFACE uses an Ornstein-Uhlenbeck (OU)
484 stabilizing selection model of evolution, which allows changes in the rate of evolution and optimal
485 means of variables. If present, this method identifies homoplasy: two clades with the same regime.
486 Given the small sample of appendages in our comparisons, we deemed it necessary to calculate the
487 power of the SURFACE analysis as an indicator of reliability in the accuracy of estimated patterns.
488 Because in OU models power is dependent by strength, rate, and optimal mean combined, effect-
489 size measures offer a better prediction of power than sample size⁶⁰. We calculated the power of the
490 estimated regimes using the Signal-to-Noise Ratio (SNR), which is defined as $SNR = \sqrt{2T}\alpha\theta/\sigma^2$,
491 where T is the total depth of the phylogeny. High power can be inferred when $SNR \gg 1$. To further
492 validate the estimated regimes, the output of SURFACE was then fitted to alternative evolutionary
493 models: a 1-rate Brownian Motion (BM); a multi-rate BM; an OU with fixed strength, rate, and
494 mean; an OU with fixed strength and rate, and multi-mean; and an OU with fixed strength, and
495 multi-rate and multi-mean. Fitted models were compared using Akaike Information Criteria.
496 Finally, we statistically tested the resulting evolutionary models of evolution with a phylogenetic
497 MANOVA to confirm that the clades identified had a different regime corresponding to different
498 groups with different means. The combination of estimation, fitting, and testing allowed us to build
499 confidence that the evolutionary patterns found were reliable if they converged on the same result.
500 Evolutionary modelling was carried out in R using functions from the packages *surface*⁵⁹,
501 *mvMORPH*⁶¹, and *geiger*⁶² for the estimation, fitting, and testing, respectively.

502

503 **Disparity through time (DTT).** To examine how topological disparity changed over time, we
504 performed a disparity through time (DTT) analysis on pectoral and pelvic appendages, separately.
505 Following a previous study on mammalian neck anatomy⁶³, first we obtained the co-variation of
506 topological variables by performing independent PCAs for pectoral and pelvic networks. Next, we
507 calculated the mean subclade disparity on the PC scores using the function *dtt* in the R package

508 *geiger*⁶². The higher the disparity, the higher the variance within subclades (i.e., lower conservation)
509 and the lower the variance between subclades^{64,65}. We tested the statistical significance of the
510 observed disparity with a randomization inference test with 10,000 simulations under a Brownian
511 motion evolution on our phylogeny. Probability values were calculated empirically at each subclade
512 time and combined using Edgington's method⁶⁶ as implemented in the R package *metap*⁶⁷. Function
513 *dtt* also calculated the morphological disparity index, which quantified the overall difference in
514 relative disparity of a clade compared to that expected under the null Brownian motion model. For
515 reference, DTT analyses were also performed on the subsample of taxa for which we have both
516 pectoral and pelvic appendages.

517

518 **Pectoral-pelvic similarity bottleneck.** We tested the hypothesis of the existence of a pectoral-
519 pelvic similarity bottleneck at the origin of Tetrapoda for each topological variable independently.
520 For practical purposes we used pectoral-pelvic disparity (lower disparity means greater similarity).
521 Pectoral-pelvic disparity was calculated as the absolute residuals of pectoral and pelvic values on
522 the identity line (or 1:1 line, a line with intercept=0 and slope=1), so that identical pelvic and
523 pectoral appendages—maximal similarity—had a value of zero disparity. According to previous
524 formulations of the bottleneck hypothesis for tetrapods, taxa before and after the split of tetrapods
525 would have a greater pectoral-pelvic disparity (lower similarity) than taxa closer to the origin of
526 tetrapods^{7,22,25}. Thus, the farther we go in time from this event the greater the expected pectoral-
527 pelvic disparity should be. To test this prediction, we performed a phylogenetic generalized least
528 square regression (PGLS) of the absolute pectoral-pelvic residuals on the 1:1 line against the time
529 from the Tetrapoda branch of taxa having both appendages in the sample ($t_0=370.4$ My). We used
530 PGLS to test against the null hypothesis of a slope=0, meaning no difference in pectoral-pelvic
531 disparity through time. For our prediction to hold, pGLS needed to show a statistically significant
532 positive regression slope. PGLS was computed in R using a standard generalized least-square with
533 an *a priori* correlation structure derived from the phylogenetic tree using the function *corPageI* of
534 the package *ape*⁶⁸.

535

536

537 **ACKNOWLEDGEMENTS**

538 We thank Jennifer Clack, Timothy Smithson, Michael Coates, and Roger Benson for their help
539 interpreting skeletal anatomy in fossil specimens. John Hutchinson's team at RVC is thanked for
540 their input on early drafts. We thank Jeroen Smaers for his teaching and insight on phylogenetic
541 analyses. We also thank Jessica Cundiff (Museum of Comparative Zoology at Harvard) and Emma
542 Bernard (Natural History Museum of London) for their assistance in accessing specimens. This

543 project is funded by the European Union's Horizon 2020 research and innovation program under
544 the Marie Skłodowska-Curie grant agreement No 654155.

545

546

547 **Reporting Summary:** Further information on experimental design is available in the Nature
548 Research Reporting Summary linked to this article.

549

550

551 **Data Availability:** The data that support the findings of this study are available from Figshare at
552 <https://figshare.com/s/4c3a1dd62d1f55728a0e>.

553

554

555 **Code Availability:** The code that support the findings of this study are available from Figshare at
556 <https://figshare.com/s/4c3a1dd62d1f55728a0e>.

557

558

559 **Competing Interests:** The authors declare no competing interests.

560

561

562 **Materials & Correspondence:** Borja Esteve-Altava, boresal@gmail.com

563

564

565 **Author Contributions**

566 BE-A, SEP, JRH: Built and revised the adjacency matrices for extinct taxa

567 BE-A, JLM, PJ, JRH, RD: Built and revised the adjacency matrices for extant taxa

568 BE-A: designed the study, analysed the networks, and wrote the manuscript.

569 All authors discussed the results and revised the manuscript.

570

571

572

573

574

575

576

577

578 **TABLES**

579 **Table 1. Values of network variables measured on each network model.**

Appendage	Taxa	N	K	D	C	L	H	A	P
Pectoral	<i>Mus</i>	33	45	0.085	0.141	4.051	0.589	0.234	0.815
	<i>Didelphis</i>	32	42	0.085	0.162	4.383	0.554	0.461	0.840
	<i>Iguana</i>	38	47	0.067	0.119	5.212	0.495	0.545	0.861
	<i>Sphenodon</i>	37	47	0.071	0.133	5.240	0.496	0.613	0.844
	<i>Seymouria</i>	40	54	0.069	0.192	5.232	0.483	0.537	0.845
	<i>Ambystoma</i>	25	35	0.117	0.181	3.870	0.515	0.542	0.778
	<i>Salamandra</i>	25	34	0.113	0.157	4.000	0.526	0.553	0.816
	<i>Eryops</i>	32	50	0.101	0.269	4.327	0.525	0.503	0.779
	<i>Balanerpeton</i>	32	42	0.085	0.103	4.669	0.472	0.659	0.848
	<i>Tulerpeton</i>	42	47	0.055	0.060	5.898	0.439	0.515	0.867
Pelvic	<i>Tiktaalik</i>	21	20	0.095	0	4.105	0.619	-0.322	0.744
	<i>Gogonasmus</i>	14	14	0.154	0.107	3.571	0.480	-0.126	0.653
	<i>Eusthenopteron</i>	14	15	0.165	0.179	3.374	0.479	-0.111	0.653
	<i>Sauripterus</i>	31	32	0.069	0.097	4.445	0.558	-0.199	0.795
	<i>Neoceratodus</i>	54	65	0.045	0.262	5.947	0.817	-0.595	0.854
	<i>Latimeria</i>	23	34	0.134	0.421	3.609	0.461	-0.121	0.783
	<i>Polypterus</i>	46	65	0.063	0.070	3.329	0.908	-0.134	0.851
	<i>Mus</i>	34	46	0.082	0.150	4.415	0.593	0.271	0.834
	<i>Didelphis</i>	33	38	0.072	0.097	4.801	0.526	0.395	0.872
	<i>Iguana</i>	30	32	0.074	0.078	5.271	0.403	0.499	0.796
Pelvic	<i>Sphenodon</i>	31	36	0.077	0.122	4.910	0.514	0.398	0.849
	<i>Westlothiana</i>	37	45	0.068	0.092	5.342	0.470	0.466	0.855
	<i>Seymouria</i>	39	54	0.073	0.214	5.285	0.486	0.619	0.838
	<i>Ambystoma</i>	32	44	0.089	0.206	4.518	0.522	0.538	0.820
	<i>Salamandra</i>	32	42	0.085	0.170	4.669	0.491	0.630	0.820
	<i>Eryops</i>	37	50	0.075	0.128	4.946	0.515	0.574	0.852
	<i>Balanerpeton</i>	38	54	0.077	0.215	4.761	0.508	0.464	0.848
	<i>Tulerpeton</i>	46	57	0.055	0.086	5.895	0.487	0.571	0.851
	<i>Ichthyostega</i>	45	53	0.054	0.101	5.890	0.505	0.595	0.866
	<i>Acanthostega</i>	40	43	0.055	0.071	5.247	0.441	0.292	0.848
582	<i>Eusthenopteron</i>	9	8	0.222	0.000	2.556	0.547	-0.385	0.642
	<i>Neoceratodus</i>	63	84	0.043	0.375	5.469	0.967	-0.711	0.799
	<i>Latimeria</i>	22	33	0.143	0.291	2.814	0.554	0.164	0.764
	<i>Polypterus</i>	8	7	0.250	0	2.107	0.794	-0.587	0.625

580 N, number of nodes; K, number of links; D, density of connections; C, mean clustering coefficient;

581 L, mean path length; H, heterogeneity of connections; A, assortativity; P, parcellation.

582

583

584

585

586

587

588 REFERENCES

- 589 1. Ahlberg, P. E. & Milner, A. R. The origin and early diversification of tetrapods. *Nature* **368**, 507–
590 514 (1994).
- 591 2. Shubin, N., Tabin, C. & Carroll, S. Fossils, genes and the evolution of animal limbs. *Nature* **388**,
592 639–648 (1997).
- 593 3. Coates, M. I., Jeffery, J. E. & Ruta, M. Fins to limbs: what the fossils say. *Evol. Dev.* **4**, 390–401
594 (2002).
- 595 4. Hall, B. K. *Fins into limbs: evolution, development, and transformation*. (University of Chicago
596 Press, 2006).
- 597 5. Clack, J. A. The fin to limb transition: new data, interpretations, and hypotheses from
598 paleontology and developmental biology. *Annu. Rev. Earth Planet. Sci.* **37**, 163–179 (2009).
- 599 6. Clack, J. A. *Gaining ground: the origin and evolution of tetrapods*. (Indiana University Press,
600 2012).
- 601 7. Diogo, R., Linde-Medina, M., Abdala, V. & Ashley-Ross, M. A. New, puzzling insights from
602 comparative myological studies on the old and unsolved forelimb/hindlimb enigma. *Biol. Rev.
603 Camb. Philos. Soc.* **88**, 196–214 (2013).
- 604 8. Amaral, D. B. & Schneider, I. Fins into limbs: recent insights from sarcopterygian fish. *Genesis*
605 **56**, e23052 (2018).
- 606 9. Pierce, S. E., Hutchinson, J. R. & Clack, J. A. Historical perspectives on the evolution of
607 tetrapodomorph movement. *Integr. Comp. Biol.* **53**, 209–223 (2013).
- 608 10. Onimaru, K., Marcon, L., Musy, M., Tanaka, M. & Sharpe, J. The fin-to-limb transition as
609 the re-organization of a Turing pattern. *Nat. Commun.* **7**, 11582 (2016).
- 610 11. Andrews, S. M. & Westoll, T. S. IX.—The postcranial skeleton of *Ensthenopteron foordi*
611 Whiteaves. *Earth Environ. Sci. Trans. R. Soc. Edinb.* **68**, 207–329 (1970).

612 12. Shubin, N. H., Daeschler, E. B. & Jenkins Jr, F. A. The pectoral fin of *Tiktaalik roseae* and
613 the origin of the tetrapod limb. *Nature* **440**, 764–771 (2006).

614 13. Holland, T. Pectoral girdle and fin anatomy of *Gogonasus andrewsae* Long, 1985:
615 implications for tetrapodomorph limb evolution. *J. Morphol.* **274**, 147–164 (2013).

616 14. Yano, T. & Tamura, K. The making of differences between fins and limbs. *J. Anat.* **222**,
617 100–113 (2013).

618 15. Gaffney, E. S. Tetrapod monophyly: a phylogenetic analysis. *Bull. Carnegie Mus. Nat. Hist.*
619 **13**, 92–105 (1979).

620 16. Wagner, G. P. & Chiu, C.-H. The tetrapod limb: a hypothesis on its origin. *J. Exp. Zool.* **291**,
621 226–240 (2001).

622 17. Shubin, N. The evolution of paired fins and the origin of tetrapod limbs. in *Evolutionary*
623 *Biology* 39–86 (Springer, Boston, MA, 1995). doi:10.1007/978-1-4615-1847-1_2

624 18. Davis, M. C. The deep homology of the autopod: insights from hox gene regulation. *Integr.*
625 *Comp. Biol.* **53**, 224–232 (2013).

626 19. Wagner, G. P. The biological homology concept. *Annu. Rev. Ecol. Syst.* **20**, 51–69 (1989).

627 20. Coates, M. I. & Cohn, M. J. Fins, limbs, and tails: outgrowths and axial patterning in
628 vertebrate evolution. *BioEssays* **20**, 371–381 (1998).

629 21. Sears, K. E., Capellini, T. D. & Diogo, R. On the serial homology of the pectoral and pelvic
630 girdles of tetrapods. *Evolution* **69**, 2543–2555 (2015).

631 22. Esteve-Altava, B., Molnar, J. L., Johnston, P., Hutchinson, J. R. & Diogo, R. Anatomical
632 network analysis of the musculoskeletal system reveals integration loss and parcellation boost
633 during the fins-to-limbs transition. *Evolution* **72**, 601–618 (2018).

634 23. Ahlberg, P. E. Paired fin skeletons and relationships of the fossil group Porolepiformes
635 (Osteichthyes: Sarcopterygii). *Zool. J. Linn. Soc.* **96**, 119–166 (1989).

636 24. Coates, M. I. & Cohn, M. J. Vertebrate axial and appendicular patterning: the early
637 development of paired appendages. *Am. Zool.* **39**, 676–685 (1999).

638 25. Diogo, R. & Molnar, J. Comparative anatomy, evolution, and homologies of tetrapod
639 hindlimb muscles, comparison with forelimb muscles, and deconstruction of the forelimb-
640 hindlimb serial homology hypothesis. *Anat. Rec.* **297**, 1047–1075 (2014).

641 26. Muller, G. B. & Wagner, G. P. Novelty in evolution: restructuring the concept. *Annu. Rev.*
642 *Ecol. Syst.* **22**, 229–256 (1991).

643 27. Polly, P. D. Developmental dynamics and G-matrices: can morphometric spaces be used to
644 model phenotypic evolution? *Evol. Biol.* **35**, 83 (2008).

645 28. Esteve-Altava, B., Marugán-Lobón, J., Botella, H. & Rasskin-Gutman, D. Network models
646 in anatomical systems. *J. Anthropol. Sci.* **89**, 175–184 (2011).

647 29. Rasskin-Gutman, D. & Esteve-Altava, B. Connecting the dots: anatomical network analysis
648 in morphological evo-devo. *Biol. Theory* **9**, 178–193 (2014).

649 30. Ruta, M., Wills, M. A. & Johanson, Z. Comparable disparity in the appendicular skeleton
650 across the fish–tetrapod transition, and the morphological gap between fish and tetrapod
651 postcrania. *Palaeontology* **59**, 249–267 (2016).

652 31. Brigandt, I. & Love, A. C. Evolutionary novelty and the evo-devo synthesis: field notes.
653 *Evol. Biol.* **37**, 93–99 (2010).

654 32. Wagner, G. P. & Lynch, V. J. Evolutionary novelties. *Curr. Biol.* **20**, R48–R52 (2010).

655 33. Brigandt, I. & Love, A. C. Conceptualizing evolutionary novelty: moving beyond
656 definitional debates. *J. Exp. Zoolog. B Mol. Dev. Evol.* **318**, 417–427

657 34. Sordino, P., van der Hoeven, F. & Duboule, D. Hox gene expression in teleost fins and the
658 origin of vertebrate digits. *Nature* **375**, 678–681 (1995).

659 35. Johanson, Z. *et al.* Fish fingers: digit homologues in sarcopterygian fish fins. *J. Exp. Zoolog.*
660 *B Mol. Dev. Evol.* **308**, 757–768 (2007).

661 36. Shubin, N., Tabin, C. & Carroll, S. Deep homology and the origins of evolutionary novelty.
662 *Nature* **457**, 818–823 (2009).

663 37. Woltering, J. M., Noordermeer, D., Leleu, M. & Duboule, D. Conservation and divergence
664 of regulatory strategies at Hox Loci and the origin of tetrapod digits. *PLoS Biol.* **12**, e1001773
665 (2014).

666 38. Nakamura, T., Gehrke, A. R., Lemberg, J., Szymaszek, J. & Shubin, N. H. Digits and fin
667 rays share common developmental histories. *Nature* **537**, 225–228 (2016).

668 39. Wainwright, P. C. Functional versus morphological diversity in macroevolution. *Annu. Rev.*
669 *Ecol. Evol. Syst.* **38**, 381–401 (2007).

670 40. Wagner, G. P. Evolutionary innovations and novelties: let us get down to business! *Zool.*
671 *Anz. - J. Comp. Zool.* **256**, 75–81 (2015).

672 41. Niedźwiedzki, G., Szrek, P., Narkiewicz, K., Narkiewicz, M. & Ahlberg, P. E. Tetrapod
673 trackways from the early Middle Devonian period of Poland. *Nature* **463**, 43–48 (2010).

674 42. Clack, J. A. Devonian tetrapod trackways and trackmakers; a review of the fossils and
675 footprints. *Palaeogeogr. Palaeoclimatol. Palaeoecol.* **130**, 227–250 (1997).

676 43. Williams, E. A., Sergeev, S. A., Stössel, I. & Ford, M. An Eifelian U-Pb zircon date for the
677 Enagh Tuff Bed from the Old Red Sandstone of the Munster Basin in NW Iveragh, SW Ireland.
678 *J. Geol. Soc.* **154**, 189–193 (1997).

679 44. Wake, D. B. Homoplasy: the result of natural selection, or evidence of design limitations?
680 *Am. Nat.* **138**, 543–567 (1991).

681 45. Young, N. M., Wagner, G. P. & Hallgrímsson, B. Development and the evolvability of
682 human limbs. *Proc. Natl. Acad. Sci. U. S. A.* **107**, 3400–3405 (2010).

683 46. Anderson, P. S. L., Friedman, M. & Ruta, M. Late to the table: diversification of tetrapod
684 mandibular biomechanics lagged behind the evolution of terrestriality. *Integr. Comp. Biol.* **53**,
685 197–208 (2013).

686 47. Diogo, R. Muscles versus bones: catfishes as a case study for a discussion on the relative
687 contribution of myological and osteological features in phylogenetic reconstructions. *Anim. Biol.*
688 **54**, 373–391 (2004).

689 48. Diogo, R. & Wood, B. Soft-tissue anatomy of the primates: phylogenetic analyses based on
690 the muscles of the head, neck, pectoral region and upper limb, with notes on the evolution of
691 these muscles. *J. Anat.* **219**, 273–359 (2011).

692 49. Molnar, J. L., Rui, D., Hutchinson, J. R. & Pierce, S. E. Reconstructing pectoral
693 appendicular muscle anatomy in fossil fish and tetrapods over the fins-to-limbs transition. *Biol.*
694 *Rev.* **93**, 1077–1107 (2017).

695 50. R Core Team. *R: A language and environment for statistical computing*. (R Foundation for
696 Statistical Computing, 2017).

697 51. Csardi, G. & Nepusz, T. The igraph software package for complex network research.
698 *InterJournal Complex Syst.* **1695**, 1–9 (2006).

699 52. Ruta, M., Coates, M. I. & Quicke, D. L. J. Early tetrapod relationships revisited. *Biol. Rev.*
700 *Camb. Philos. Soc.* **78**, 251–345 (2003).

701 53. Coates, M. I., Ruta, M. & Friedman, M. Ever since Owen: changing perspectives on the
702 early evolution of tetrapods. *Annu. Rev. Ecol. Evol. Syst.* **39**, 571–592 (2008).

703 54. Hedges, S. B. & Kumar, S. *The timetree of life*. (Oxford University Press, 2009).

704 55. Brusatte, S. L., Benton, M. J., Ruta, M. & Lloyd, G. T. Superiority, competition, and
705 opportunism in the evolutionary radiation of dinosaurs. *Science* **321**, 1485–1488 (2008).

706 56. Lloyd, G. T., Wang, S. C. & Brusatte, S. L. Identifying heterogeneity in rates of
707 morphological evolution: discrete character change in the evolution of lungfish (Sarcopterygii;
708 Dipnoi). *Evol. Int. J. Org. Evol.* **66**, 330–348 (2012).

709 57. Bapst, D. W. paleotree: an R package for paleontological and phylogenetic analyses of
710 evolution. *Methods Ecol. Evol.* **3**, 803–807 (2012).

711 58. Oksanen, J. *et al.* *vegan: Community Ecology Package*. (R Foundation for Statistical
712 Computing, 2018).

713 59. Ingram, T. & Mahler, D. L. SURFACE: detecting convergent evolution from comparative
714 data by fitting Ornstein-Uhlenbeck models with stepwise Akaike Information Criterion. *Methods*
715 *Ecol. Evol.* **4**, 416–425

716 60. Cressler, C. E., Butler, M. A. & King, A. A. Detecting adaptive evolution in phylogenetic
717 comparative analysis using the Ornstein-Uhlenbeck model. *Syst. Biol.* **64**, 953–968 (2015).

718 61. Clavel, J., Escarguel, G. & Merceron, G. mvmorph: an r package for fitting multivariate
719 evolutionary models to morphometric data. *Methods Ecol. Evol.* **6**, 1311–1319

720 62. Harmon, L. J., Weir, J. T., Brock, C. D., Glor, R. E. & Challenger, W. GEIGER:
721 investigating evolutionary radiations. *Bioinforma. Oxf. Engl.* **24**, 129–131 (2008).

722 63. Arnold, P., Esteve-Altava, B. & Fischer, M. S. Musculoskeletal networks reveal topological
723 disparity in mammalian neck evolution. *BMC Evol. Biol.* **17**, 251 (2017).

724 64. Harmon, L. J., Schulte, J. A., Larson, A. & Losos, J. B. Tempo and mode of evolutionary
725 radiation in iguanian lizards. *Science* **301**, 961–964 (2003).

726 65. Slater, G. J., Price, S. A., Santini, F. & Alfaro, M. E. Diversity versus disparity and the

727 radiation of modern cetaceans. *Proc. R. Soc. Lond. B Biol. Sci.* rspb20100408 (2010).

728 66. Edgington, E. S. An additive method for combining probability values from independent

729 experiments. *J. Psychol.* **80**, 351–363 (1972).

730 67. Dewey, M. *Metap: meta-analysis of significance values.* (2018).

731 68. Paradis, E., Claude, J. & Strimmer, K. APE: analyses of phylogenetics and evolution in R

732 language. *Bioinformatics* **20**, 289–290 (2004).

733